

Volume and surface photoemission processes from plasmon resonance fields*

T. A. Callcott

Department of Physics, University of Tennessee, Knoxville, Tennessee 37916

E. T. Arakawa

Health Physics Division, Oak Ridge National Laboratory, Oak Ridge, Tennessee 37830

(Received 4 September 1974)

Photo yield was measured as a function of incident angle for polarized light incident through a MgF_2 semicylinder onto thin ($\sim 200\text{-}\text{\AA}$) films of Al. Photon energies from threshold at 4.8 up to 10.2 eV were used. For p -polarized light near threshold, a surface-plasmon resonance peak was observed at about 50° from normal incidence with yields more than 100 times those at normal incidence. If the yield at normal incidence is assumed to result from pure volume photoemission, the angular yield ratio $Y(\theta)/Y(0)$ can be calculated for the volume process. Only $(35 \pm 10)\%$ of the yield observed at the plasmon peak could be accounted for by the volume process. The remaining yield was attributed to the surface emission process. The ratios of yields from Al with light normally incident from vacuum and through the MgF_2 substrate were analyzed to obtain values of the escape depths for the volume process. Escape lengths were determined ranging from $45 \pm 15 \text{ \AA}$ for 5-eV electrons to $20 \pm 10 \text{ \AA}$ for 8.2-eV electrons.

INTRODUCTION

Light of p polarization obliquely incident on a thin metal film through a transparent substrate of higher index of refraction may be used to generate a surface-plasma oscillation on the vacuum surface of the film. The presence of the resonance strongly affects both the optical and photoemissive properties of the film. As the angle of photon incidence is varied, there is a strong dip in the reflectance and a large increase in the photoemission. Studies of the optical generation of surface plasmons have been reported by Otto¹ and Kretschmann.² Arakawa *et al.*,³ have used the angular position of the dip in reflectance to map out the frequency versus wave vector curve of the surface-plasma resonance of Ag. Braundmeier and Arakawa⁴ have discussed the effect of surface roughness on resonance absorption in Ag. Macek *et al.*⁵ have reported both optical and photoemission measurements on Al for light of 5-eV photon energy.

In this paper we report photoemission measurements on films of aluminum for angles of 0° to 80° with light incident both from vacuum and through the substrate. Data were obtained for photon energies between 4.8 and 5.8 eV, near the threshold for photoemission, and at higher energies between 7.7 and 10.2 eV. The photoemission yield at the plasmon resonance was analyzed to obtain an estimate of the relative strength of surface and volume photoemission processes in the energy region near threshold. The ratio of photoyield with light incident from vacuum and through the substrate was analyzed to determine the escape

depth for electrons produced by the volume process.

The plasmon resonance may be understood qualitatively as follows. On a smooth surface, light will couple to the surface resonance only when it contains transverse field components at the surface with the same wave vector (or wavelength) and frequency as the surface-plasmon fields. Thus a light wave propagating outside a metallic surface does not couple to the surface plasmon because its wave vector is always smaller than the plasmon wave vector of equal energy. In other language, the ω -vs- k dispersion curve of the surface plasmon always lies to the right of the vacuum light line, as illustrated in Fig. 1 for a free-electron gas with the carrier density of Al. However, the wave vector of light propagating in a transparent medium of index of refraction n , has a wave vector given by $k_n = nk_0$, where k_0 is the wave vector in vacuum. For most optical materials $n \approx 1.5$ and k_n is greater than the plasmon wave vector in the retarding region of the plasmon dispersion curve. In our experiment, light is incident through a semicylinder of MgF_2 as in Fig. 2. At a particular angle θ_p , the tangential component of k_n given by $k_T = nk_0 \sin \theta_p$ just matches the plasmon wave vector on the *vacuum* interface of the metal film. When the metal film is sufficiently thin ($\approx 250 \text{ \AA}$), optical fields penetrating the film resonate with the surface-plasmon fields. Coupling occurs only for p -polarized light which, for nonzero angles of incidence, contains a component of electric field perpendicular to the film surface.

Except in a region of 1 or 2 \AA at the surface,

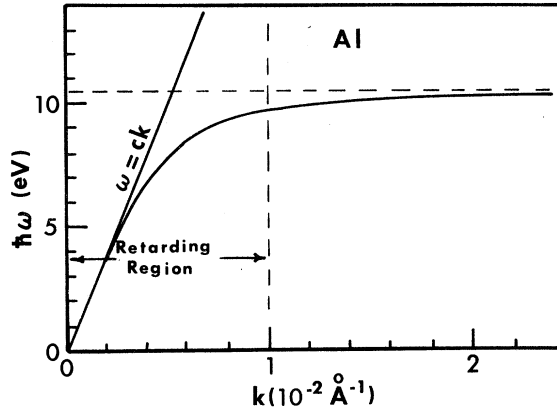


FIG. 1. Plasmon dispersion curve for a free-electron gas with the electron density of aluminum.

the electric fields associated with the resonance are correctly described by Fresnel's equations for a smooth-surfaced thin film bounded by vacuum and MgF_2 . In our analysis, Fresnel's equations are used to calculate the electric fields generating volume photoemission in the samples.

In early studies of metals, photoemission was interpreted as a surface process in which electrons were excited directly from initial states in the metal to final states in vacuum, with momentum normal to the surface being conserved by interaction with the surface potential barrier. More recently, photoemission has usually been interpreted as a volume effect in which optical excitation in the bulk is followed by transport to and escape through the surface. Very recently Endriz and Spicer⁶ have published data and Endriz⁷ has published calculations which suggest that, for electric-field components normal to the surface, the surface effect is dominant in aluminum for photon energies below about 10 eV, with the volume effect being dominant at higher energies.

The relative importance of the two processes cannot be investigated by comparing experimental and theoretical values of absolute photoyield because of uncertainties in the calculations. The most promising method of differentiating surface and volume effects is to exploit the fact that the surface effect can only be generated on a smooth surface by electric-field components normal to the surface, while the volume effect may be excited by transverse components as well. Thus photoemission with photons incident normally on the surface should produce only volume photoemission while photons incident at oblique angles may excite both processes. The situation is more complicated for photon energies near the high- k plasmon energies (~ 10.5 eV in Al) where surface roughness couples even normally incident photons

to the surface plasmon.^{6,8,9} However, this coupling is inefficient in the retarding region compared with the direct optical coupling used in these experiments.

A rigorous test may be made using the fields associated with surface plasmons, which Endriz showed to be uniquely effective in generating the surface photoeffect. In a later section of this paper, we evaluate parameters of the volume theory from the photoyield produced from Al by photons normally incident through the substrate, and use these parameters to calculate the photoyield at all angles including the plasmon-resonance angle. The result is that only about 35% of the observed yield at the plasmon resonance peak may be attributed to an isotropic volume photoeffect, the remainder being due to a surface effect. The only alternative explanation of the data is that components of the electric field normal to the surface are many times more effective in generating volume photoemission than are the transverse fields. This explanation does not seem likely.

One of the important parameters in models of the volume photoemission process is the escape depth L for photoexcited electrons. At photon energies near threshold L , as it appears in expressions for the photoyield, is essentially a direct measure of the scattering length for hot electrons. At higher energies, the scattering length

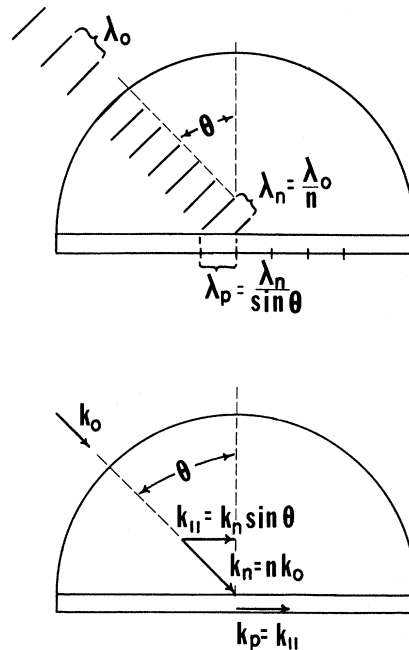


FIG. 2. Matching conditions on wavelength and wave vector for generation of surface plasmons.

may be determined from L , if the theory is applied only to the partial yield of the most energetic electrons. By measuring the ratio of measurements of yield with photons incident from the front and from the back of a thin film, we may eliminate uncertainties from poorly known excitation and escape probabilities and calculate L in terms of the relative yields and the optical constants of the system. Using this method we have calculated scattering lengths for hot electrons with energies between 5 and 10 eV.

EXPERIMENTAL METHODS

All experiments were performed in an ion-pumped ultrahigh-vacuum system. Samples were prepared as thin films evaporated onto the 1-in. \times 2-in. surface of a semicylinder of MgF_2 . Before pumpdown the substrate was cleaned with KOH to remove Al, rinsed in distilled water and propanol, and vapor cleaned in freon. After outgassing with a shutter in place, 99.999% aluminum was evaporated from a tungsten filament. Pressure, as measured by an ion gauge in the experimental chamber, was $(1-5) \times 10^{-7}$ Torr during evaporation and $(1-3) \times 10^{-9}$ Torr during measurements. Film thickness was determined by measuring the normal incidence transmission at $\lambda = 5480 \text{ \AA}$ using a photomultiplier mounted opposite the light source. Thickness was read off transmission-versus-thickness curves previously measured at Oak Ridge National Laboratory (ORNL).¹⁰ In experiments where the film thickness was an important parameter, the thickness determination was checked with an optical interference microscope after the film was removed from the chamber.

A prism monochromator with a high-pressure Hg-xenon lamp as source was used for excitation at photon energies below 5.2 eV. A 0.5-m Seya monochromator with a hydrogen discharge lamp as source was used for excitation for photon energies between 7.7 and 10.2 eV.

Both yields and energy distributions of emitted electrons were measured. Energy distributions were measured using the standard retarding-potential method in which the energy distribution is plotted directly after electronic differentiation of the current-versus-retarding-voltage curves. The energy resolution varied between 0.2 and 0.4 eV in the experiments. The retarding potential can was slotted so that light specularly reflected from the sample passed out of the can without exciting significant back emission. This was particularly important when measuring partial yields due to the most energetic electrons excited by the higher photon energies. Partial-yield mea-

surements were made to determine values of the escape depth appropriate to the most energetic electrons.

In some experiments, the yields were measured as the semicylinder was continuously rotated so that its value was determined for all angles with photons incident both from vacuum and through the substrate, except for angles between 80° and 90° from the normals where the semicylinder support blocked the beam. Absolute angle assignments are accurate to at least $\frac{1}{2}^\circ$. The use of a semicylinder as substrate assures that the interfaces and path lengths are the same for all angles of incidence when the light enters and is reflected through the substrate. Using continuous rotation of the sample, angular photoyields could be obtained with photocurrent down to about 5×10^{-11} A. For lower total photocurrents, excessive noise due to vibration of the sample mount and leads made it necessary to take point-by-point measurements.

COMPARISON OF ANGULAR YIELDS TO VOLUME-PHOTOEMISSION CALCULATIONS

Angular-yield measurements $Y(\theta)$ made with light incident through the substrate are shown in Figs. 3 and 4. The data for photon energies near threshold (Fig. 3) were measured using p -polarized light incident on a $235 \pm 15\text{-\AA}$ film. In these

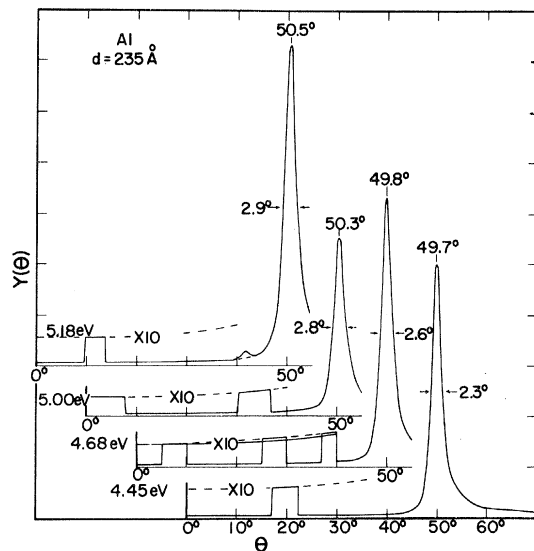


FIG. 3. Total photoyield vs incident angle of p -polarized photons for energies near threshold. Solid curves are traces from original data. Some portions of each curve were taken at $\times 10$ magnification. Curves are labeled with photon energies.

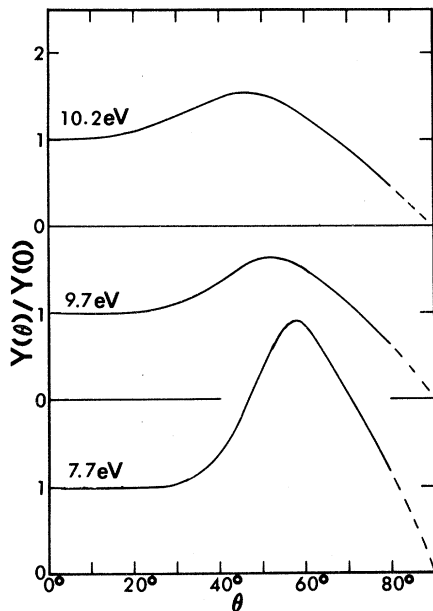


FIG. 4. Total photoyield vs incident angle of partially polarized photons of energies between 7.7 and 10.2 eV. Curves normalized to yield at normal incidence.

curves the plasma-resonance peak is located near 50° and the yield at the resonance angle is about 100 times greater than the normal-incidence yield. Some portions of each yield curve were made with $\times 10$ amplification. For 5 eV, the entire curve up to the plasmon peak was repeated with $\times 10$ amplification. Similar $Y(\theta)$ curves made with s -polarized light showed a small peak of about two times normal incidence yield at the plasmon resonance, presumably due to a 1% admixture of p -polarized light in the incident beam.

The higher energy data of Fig. 4 show the angular yields produced by partially polarized light from the Seya monochromator incident on a 120-Å film. The light is predominantly s -polarized at 10.2 eV,¹¹ and the film is thinner so that a far less spectacular resonance peak is produced. We did not find it possible to obtain polarized light of sufficient intensity with our sources. Consequently, most of our analysis has been applied to the low-energy data of Fig. 3.

We wish to determine what portion of the photoemission excited by obliquely incident photons may be attributed to the volume process, assuming that all photoemission by normally incident photons is volume emission. Several authors have developed theories which give the volume photoyield from a thin film with optical constants n_1 and k_1 (or dielectric constants ϵ_1 and ϵ_2) bounded by a transparent dielectric ($n_2 > 1$, $k_2 = 0$) and by vacuum $n_0 = 1$, $k_0 = 0$).¹²⁻¹⁴ In these calcula-

tions, the energy density of the exciting field, $\eta(y)$, is calculated as a function of the distance y from the vacuum interface. The density η depends on the optical constants of the film and substrate (n_1, k_1, n_2), on the polarization and incident angle of the photons and on the film thickness d . The optical constants are of course functions of photon energy. Excitation is assumed to be isotropic, as would be the case for a free-electron metal, and to be independent of the direction of the electric field vector of the incident photons. The parameters of the theory are illustrated in Fig. 5.

Following earlier workers,^{15,16} Coquet *et al.*¹² and Pepper¹³ described the transport process as a one-dimensional problem characterized by an escape length L . The number of electrons reaching the surface without scattering is $e^{-y/L}$, and a fixed fraction of these electrons escape. Gesell¹⁴ refined the calculation by describing three-dimensional transport in terms of a scattering length l for travel along any direction from the point of excitation. All electrons escape which reach the surface within the classical escape cone defined by $\cos \theta_{\text{esc}} = (E_v/E)^{1/2}$, where θ_{esc} is the maximum angle electrons may make with the surface normal and escape. E is the excited electron's energy and E_v the energy of the surface barrier, both measured with respect to the bottom of the conduction band. In both theories, the initial distribution of electron momenta is assumed to be isotropic, and the escape parameter is assumed to depend only on electron energy. Both theories are most logically applied to partial yields of electrons with a narrow range of energies. If the contribution of the scattered electrons to the yields are subtracted, and the analysis applied to such partial yields, both l and L give measures of the scattering length for hot electrons of a particular energy.

Near threshold, the theories may be applied to

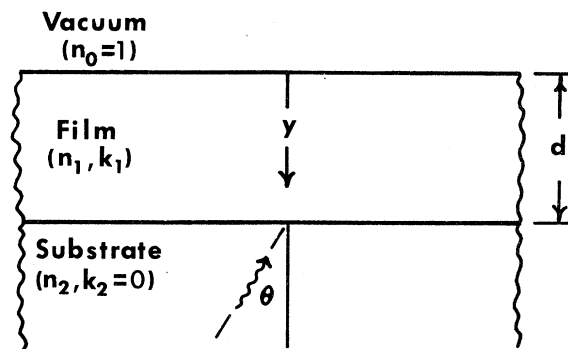


FIG. 5. Parameters used in model of the volume photoemission process.

the total yield since only electrons with a narrow range of energies escape, and few electrons retain enough energy to surmount the surface barrier after an electron-electron scattering event. The one-dimensional parameter L and the three-dimensional parameter l are related by $L \approx l \langle \cos \theta \rangle$, where $\langle \cos \theta \rangle$ is averaged over angles within the escape cone.¹⁶ For electrons near threshold $\theta_{\text{esc}} \ll \frac{1}{2} \pi$ and $L \approx l$ and both the three and one-dimensional theories take the same form. For very large energies where $\theta_{\text{esc}} \approx \frac{1}{2} \pi$, $L = \frac{1}{2} l$.¹⁶ Our data apply to electrons reasonably near threshold ($\cos \theta_{\text{esc}} \approx 0.98$ for a 5-eV electron, $\cos \theta_{\text{esc}} \approx 0.87$ for 10-eV electrons in Al). Consequently, we will use Pepper's somewhat simpler formalism. The yield with photons incident from the vacuum is

$$Y_0 = C \int_0^d e^{-y/L} \eta(y) dy = CF(L), \quad (1)$$

and with photons incident through the substrate is

$$Y_2 = C \int_0^d e^{-(d-y)/L} \eta(y) dy = CF'(-L)e^{-d/L}. \quad (2)$$

The excitation and escape factors are contained in the constant C and are the same for excitation from either side of the film. The function F depends on the same parameters as $\eta(n_0, n_1, k_1, n_2, \theta, \text{polarization}, d)$ as well as on the escape depth L . F' differs from F only in the interchange of n_0 and n_2 to account for the different incident media for the photons. Complete expressions for F are available in the literature.¹²⁻¹⁴

Using Pepper's equations, we analyzed the ratio of the yield at some angle θ , $Y_2(\theta)$, to the yield at normal incidence through the substrate, $Y_2(0)$. The excitation and escape factors cancel in the ratio $Y_2(\theta)/Y_2(0)$, leaving only the dependence on the optical constants, d , and L . Experimental values of $Y(\theta)/Y(0)$ excited by 4.68-eV p -polarized light are plotted as a solid line in Fig. 6. The ratio calculated from Eq. (2) with independently determined values of n_1, k_1, n_2, L , and d are shown as dotted lines. Values of n_1 and k_1 were taken from the literature¹⁷ and of n_2 for the MgF_2 semicylinder from ORNL data.¹⁸ We determined L to have a value of $45 \text{ \AA} \pm 15 \text{ \AA}$ by the method described below, and d was measured using methods described above. At the plasma peak, using values of $d = 235 \text{ \AA}$, $L = 40 \text{ \AA}$, the calculated ratio is 40 or about 35% of the experimental ratio. A study was made of the sensitivity of the calculated ratio at the peak to errors in L and d . Taking the extreme values of L to be 30 \AA and 60 \AA and d to be $235 \pm 15 \text{ \AA}$, the yield

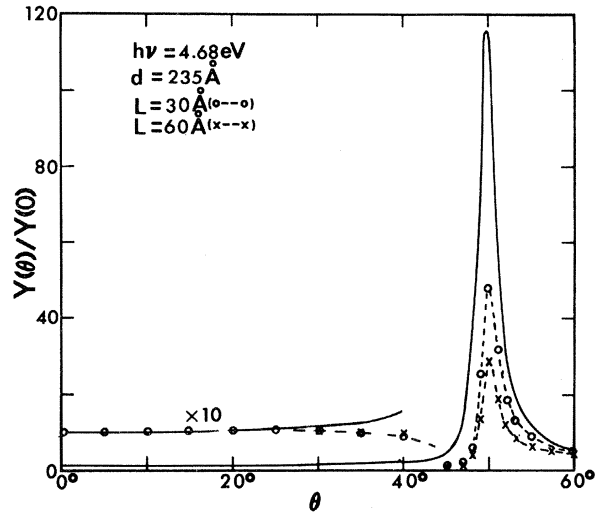


FIG. 6. Comparison of experimental values of the angular yield ratio to values calculated from the volume photoemission model. No possible choice of film thickness (d) and escape depth (L) can account for the yield observed at the resonance peak.

ratio at the plasmon peak was found to vary from 21 to 46% of the experimental ratio. The maximum ratio is obtained in the limit $L \rightarrow 0 \text{ \AA}$, where the yield ratio is equal to the energy density ratio $\eta(\theta)/\eta(0)$ at the vacuum interface. Even in this limit the volume theory only accounts for about 60% of the total emission observed in the resonance peak.

The theory should certainly give correct values of the yield ratio for the component of the electric field vector \vec{E} parallel to the sample surface. Excitation, transport, and escape should be identical for this component with normal incidence photons and at an angle θ . The component of \vec{E} normal to the surface is properly described in the theory if it produces electrons isotropically with the same efficiency as the parallel component of \vec{E} . A possible explanation of our result is that the normal component is many times more efficient at producing volume photoemission than is the parallel component. We know no reason to expect such strong vectorial effects for volume emission from polycrystalline films of a nearly free electron metal like Al. Hence we conclude that the excess photoemission at large angles, and particularly at the plasmon peak, may be attributed to the surface photoeffect, to which only the normal component of the exciting field contributes.

This result is in qualitative agreement with the calculations of Endriz which indicated that the surface emission is about five times the volume emission for surface plasmon fields in the re-

tarding region.⁷ Even though we find a smaller ratio, the agreement seems satisfactory in view of the uncertainties in Endriz's calculation and in our determination of the yield ratio.

The same analysis was applied to the other curves of Fig. 3 with essentially the same result. A similar analysis applied to the higher-energy curves of Fig. 4 was inconclusive due to a large and somewhat uncertain percentage of s-polarized light in the exciting beam.

Some additional evidence for surface emission may be obtained from an examination of the energy distribution curves (EDCs) of photoemitted electrons. We can examine the curves for evidence of scattered electrons which should be produced by the volume process, but not by the surface process. In Fig. 7 we display EDCs made at three photon energies with photons normally incident from vacuum, and with photons incident through the substrate both normally and at the resonance angle. For each energy the curves are normalized at the high-energy shoulder of the distributions. Energy distributions for photon energies just above threshold are not included because a scattered electron peak cannot be resolved. The energy resolution of the 5.2-eV curve is ≈ 0.2 and of the 7.7- and 9.7-eV curves is ≈ 0.4 eV.

The relative amount of scattering expected from the volume process for each angle of excitation may be estimated from plots of energy density $\eta(y)$ vs y such as those plotted in Fig. 8 using parameters appropriate to 5.2-eV photons incident on a 160-Å film. Profiles calculated for other

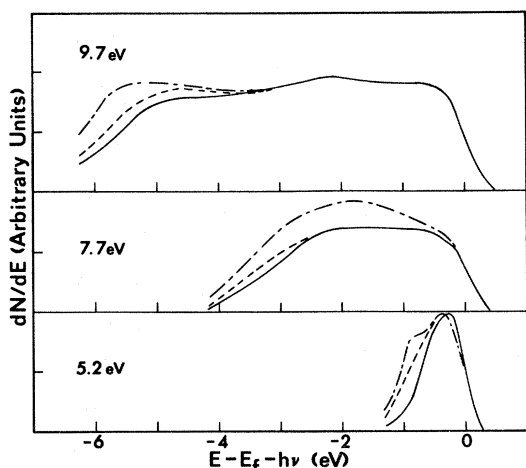


FIG. 7. Energy distributions measured with photons incident at the plasmon angle (solid line), normally through the substrate (dot-dash line), and normally from vacuum (dashed line). Each set of curves is labeled with the incident photon energy.

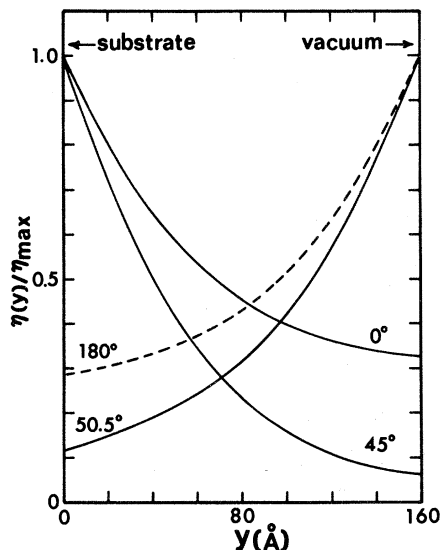


FIG. 8. Normalized energy densities in a 160-Å aluminum film for different angles of incident light. 0° labels curve for photons incident normally through the substrate. 50.5° is the plasmon-resonance angle.

photon energies have the same characteristic features. EDCs were taken with somewhat thinner Al films than those of Fig. 3 in order to obtain sufficiently large yields for energy analysis with photons normally incident through the substrate.

For normal incidence, the energy density decreases nearly exponentially away from the surface of incidence. At the plasmon resonance, it is reversed and has a profile very similar to that produced by photons incident from vacuum. At angles $\sim 5^\circ$ below the peak, the theory predicts a minimum in the photoemission which we have not observed experimentally. Clearly, relatively more electrons are produced away from the emission surface for photons normally incident through the substrate, and such excitation should produce the strongest scattering peak. The volume process should produce comparable scattering for the other two angles of excitation. In all cases, the scattering peak is largest for photons normally incident through the substrate as expected. The experimental curves indicate that there are significantly fewer scattered electrons in the plasmon-resonance photoemission than in free-surface photoemission. Though by no means conclusive, the EDCs are at least consistent with the existence of a strong surface emission at the resonance angle.

Some practical implications of the very striking resonance photoemission results deserve comment. First, we note that resonance excitation produces yields an order of magnitude greater

than vacuum surface excitation. It occurs through a substrate and thus in the geometry most useful in an evacuated phototube. Since the resonance peak occurs at very nearly the same angle for all photon energies below 5 eV, a fixed angle prism would serve as a very satisfactory substrate for films to be used in detector applications. We note also that the plasma-resonance generation extends to all lower photon energies and will enhance photoemission to much lower energies if the surface work function is lowered. Finally, a detector using such resonance enhancement would have a very narrow light-acceptance angle ($\sim 5\%$) and would be sensitive to photons of only one polarization. Sensitivity to photons outside the acceptance angle and/or of the opposite polarization is down by a factor of about 100.

THE DETERMINATION OF ESCAPE DEPTH

Previous attempts have been made to use Pepper's theory to determine the escape depth L . Gesell and Arakawa analyzed curves of the ratio $Y(\theta)/Y(0)$ vs θ for photons incident from vacuum on thin films to obtain values of L .¹⁹ In most cases, however, even though the absolute yield is a strong function of L , this ratio is not.²⁰ As we have seen above, surface emission may also be important at oblique angles.

Similar measurements have been used by Vernier *et al.* to measure L in a variety of materials using photons incident at oblique angles.²¹ Several other authors have used the yield ratio to determine L , but have used an erroneous analysis which assumes that internal reflection may be neglected. Even for films whose thicknesses are several times the absorption depth, this assumption is incorrect. With photons incident through the substrate, the first internal reflection occurs at the vacuum interface. For a highly reflecting interface such as that between Al and vacuum, the first internally reflected beam always makes an important contribution to the back yield, and hence to the yield ratio.

In Fig. 9, we plot the theoretical yield ratio $[Y_2(\theta=0)/Y_0(\theta=0)]_{\text{theor}}$ versus escape depth for film thicknesses between 75 and 250 Å. The excitation and escape factors contained in C of Eqs. (1) and (2) are the same for both front and back so that

$$[Y_2(0)/Y_0(0)]_{\text{theor}} = F'(-L)e^{-d/L}/F(L). \quad (3)$$

We previously noted that F' and F differ only in the interchange of the indices of refraction of vacuum and the substrate wherever they appear in the equations. The importance of the internal reflection is illustrated in Fig. 9 by the fact that the ratios exceed 1 for thin films; in the absence of

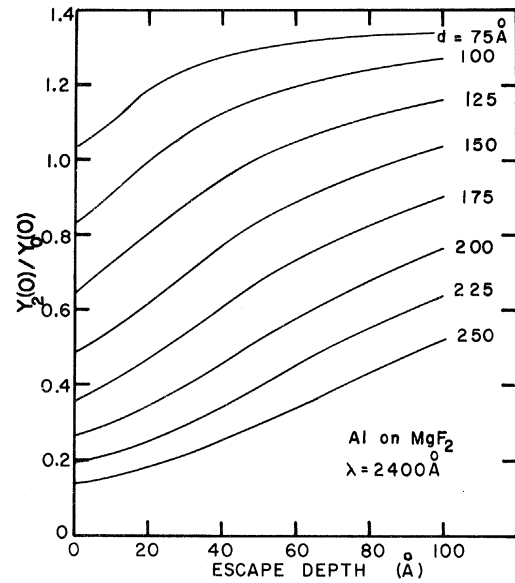


FIG. 9. Calculated ratio of photoyield with photons incident through the substrate to yield with photons incident from vacuum vs escape depth for films of thicknesses between 75 and 225 Å.

internal reflection this ratio is always less than 1.

Additional light losses associated with illumination through the substrate must be accounted for before (3) can be compared to experiment. We include a factor $(1 - R_{02})$ to account for reflection losses at the curved surface of the semicylinder and a factor (T_2) to account for transmission losses in the MgF_2 , which becomes significant for wavelengths below about 2000 Å. Our analysis then uses an equation of the form

$$[Y_2(0)/Y_0(0)]_{\text{expt}} = T_2(1 - R_{02}) F'(-L)e^{-d/L}/F(L). \quad (4)$$

Using measured values of Y_2/Y_0 for a 120-Å-thick film, independently determined values of the optical constants of Al and MgF_2 , and values of $T_2(1 - R_{02})$ determined from transmission measurements on an uncoated semicylinder, we found the values of L listed in Table I for several values of incident photon energy. The electron energies listed are mean values for the electrons contributing to the partial yields measured. The table also gives values of the other parameters used in the calculation. The major contribution to the rather large limits of error indicated for L come from the uncertainty in the determination of the film thickness.

From measurements on thicker films (~ 250 Å), we have obtained less satisfactory results, in that the yield ratios observed at the higher en-

TABLE I. Parameters used in the calculations of escape depth from the front to back yield ratio.

Photon energy (eV)	Electron energy (eV)	d (Å)	$(1-R_{02})T_2$	$\frac{Y_F}{Y_B}$ expt	n_1	k_1	n_2	L (Å)
5.2	5.0 ± 0.2	120 ± 10	0.966	1.06	0.158	2.59	1.41	45 ± 15
7.8	6.8 ± 1.0	120 ± 10	0.545	0.43	0.080	1.80	1.47	25 ± 10
9.8	8.2 ± 1.0	120 ± 10	0.275	0.22	0.060	1.20	1.59	20 ± 10

nergies are anomalously small, so that the escape depths determined from (4) are well below those listed in the table. In some cases the measured yields are even smaller than would be expected with zero escape depth.

We attribute the anomalously low values of the yield with back illumination to the presence of significant emission via the roughness-coupled surface photoeffect. This may reduce the yield ratio in two ways. Surface emission depends on the magnitude and gradient of the electric field in a very thin surface layer, (~ 1 Å). If it were proportional to the magnitude alone, it would contribute to the yield ratio in the same way as a volume theory with a ~ 1 -Å escape depth. In addition, it is known that within about 2 eV of the

surface plasmon energy (10.5 eV in Al), surface roughness may absorb sufficient energy to reduce the reflectance of the surface. The reduced internal reflection would reduce the yield ratio even for purely volume emission.

Two factors give us some confidence that the L values quoted are representative of true volume emission. Experience has shown that the roughness-coupled plasmon excitation increases with increasing film thickness, presumably because thick films are rougher.^{22,23} Of greater importance, roughness effects are greatest near the high- k surface-plasmon energy and thus should be much stronger at 10 eV than at 5 eV. This is precisely the effect we have observed in some of the thicker films but not in the films from which the values of Table I are taken.

In Fig. 10, we compare our values of the attenuation lengths with those measured by other workers and with the electron-electron scattering lengths calculated by Ashley and Ritchie for a free-electron gas with the density of aluminum. Our value of the attenuation length at 5.0 eV is in good agreement with the value obtained by Kanter²⁴ from direct measurements of the attenuation of electron beams by thin foils. They are, however, lower than values obtained by Feuerbacher *et al.*,²⁵ Pong *et al.*,²⁶ and Wooten *et al.*²⁷ from analysis of photoemission data for photon energies between 5 and 10 eV. These analyses were made using assumptions appropriate to the volume emission process and neglect surface emission. It seems probable to us that surface emission contributes in an important way to their yields and that their values are consequently too high. We have noted above that the presence of emission via the roughness-coupled surface photoeffect would affect our determination of yield in the opposite way and lead to erroneously small values.

Gesell has determined attenuation lengths in the immediately higher photon energy range by the analysis of total yield using L as an adjustable parameter.^{14, 19} Thus any unaccounted-for process which increases (or decreases) yield increases (or decreases) the value of L determined. The

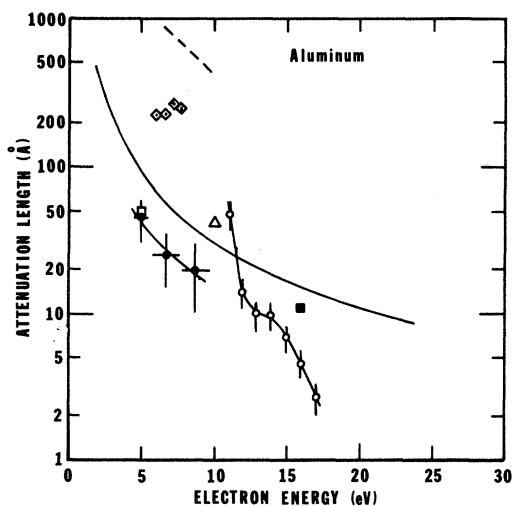


FIG. 10. Attenuation lengths for electrons in a aluminum as a function of energy above the Fermi level. Solid circle, our data; diamond with dot, Pong *et al.* (Ref. 26); dashed line, Wooten *et al.* (Ref. 27); open square, Kanter (Ref. 24); open circle, Gesell (Ref. 14) from total yield; solid square, Gesell from $Y(\theta)/Y(0)$; solid line, theory of Ritchie and Ashley with exchange correction. Bars through solid and open circles indicate estimated limits of error due to experimental uncertainties.

value of L he determines at the surface plasmon energy is significantly higher than the other values he obtained, presumably due to enhanced yield produced by the roughness-coupled surface-plasmon excitation. Above 15 eV, his values are thought to be too low; here the yield is depressed by the introduction of a new energy-loss process in which electrons lose energy by exciting surface plasmons as they approach the sample surface. Our values of L join satisfactorily to the values Gesell found in the intermediate region between 11 and 14 eV, where neither of the above processes are important, and to the single value he obtained at 16 eV from an analysis of the angular yield ratio $Y(\theta)/Y(0)$ at this energy.

Several theorists have calculated attenuation lengths for electron-electron scattering in a free-electron gas at metallic densities. The early calculation of Quinn²⁸ neglected certain exchange

corrections. Ashley and Ritchie²⁹ obtained ~40% higher values from calculations in which these corrections are included. Kleinman³⁰ evaluated the effect of making certain corrections to the energy-dependent dielectric constant and found values intermediate between those of the previous workers. Our results are in reasonable agreement with the calculations of Quinn and of Kleinman, but are significantly lower than those calculated by Ashley and Ritchie. The results of Ashley and Ritchie are plotted in Fig. 10. We note that all of these calculations are for free-electron gases and neglect any lattice effects.

ACKNOWLEDGMENTS

We acknowledge and extend thanks to R. H. Ritchie and P. Vernier for helpful discussions of the data and to R. N. Hamm for his help with the yield calculations.

*Research sponsored in part by the U. S. Atomic Energy Commission under contract with Union Carbide Corp. and in part by Defense Nuclear Agency under subtask TA 040, but does not necessarily reflect endorsement by the sponsor.

¹A. Otto, *Z. Phys.* **216**, 398 (1968); **219**, 227 (1969), *Phys. Status Solidi* **26**, K99 (1968); **42**, K37 (1970).

²E. Kretschmann, *Z. Phys.* **241**, 313 (1971); E. Kretschmann and H. Raether, *Z. Naturforsch. A* **23**, 2135 (1968).

³E. T. Arakawa, M. W. Williams, R. N. Hamm, and R. H. Ritchie, *Phys. Rev. Lett.* **31**, 1127 (1973).

⁴A. J. Braundmeier and E. T. Arakawa, *J. Phys. Chem. Solids* **35**, 517 (1974).

⁵C. Macek, A. Otto, and W. Steinmann, *Phys. Status Solidi* **51**, K59 (1972).

⁶J. G. Endriz and W. E. Spicer, *Phys. Rev. Lett.* **24**, 64 (1970).

⁷J. G. Endriz, *Phys. Rev. B* **7**, 3464 (1973).

⁸J. G. Endriz and W. E. Spicer, *Phys. Rev. B* **4**, 4144 (1971).

⁹A. Daude, A. Savary, and S. Robin, *J. Opt. Soc. Am.* **62**, 1 (1972).

¹⁰W. F. Hanson and E. T. Arakawa, ORNL Report (unpublished).

¹¹W. F. Hanson and E. T. Arakawa, *J. Opt. Soc. Am.* **56**, 124 (1966); J. J. Cowan, E. T. Arakawa, and L. R. Painter, *Appl. Opt.* **8**, 1734 (1969).

¹²E. Coquet and P. Vernier, *C. R. Acad. Sci. (Paris)* **262**, 1141 (1966).

¹³S. V. Pepper, *J. Opt. Soc. Am.* **60**, 805 (1970).

¹⁴T. F. Gesell, Ph.D. thesis (University of Tennessee, 1971) (unpublished).

¹⁵W. E. Spicer, *Phys. Rev.* **112**, 114 (1958); W. E. Spicer and F. Wooten, *Proc. IEEE* **51**, 1119 (1963).

¹⁶E. O. Kane, *Phys. Rev.* **147**, 335 (1966).

¹⁷G. Hass and J. E. Waylonis, *J. Opt. Soc. Am.* **51**, 719 (1961); H. Ehrenreich, H. R. Phillip, and B. Segall, *Phys. Rev.* **132**, 1918 (1963).

¹⁸B. L. Sowers, R. D. Birkhoff, and E. T. Arakawa, ORNL Report (unpublished).

¹⁹T. F. Gesell and E. T. Arakawa, *Phys. Rev. Lett.* **26**, 377 (1971).

²⁰E. T. Arakawa, R. N. Hamm, and M. W. Williams, *J. Opt. Soc. Am.* **63**, 1131 (1973).

²¹P. J. Vernier, J. P. Goudonnet, G. Chabrier, J. Cornaz, *J. Opt. Soc. Am.* **61**, 1065 (1971); also G. Chabrier, J. P. Goudonnet, J. F. Truitard and P. Vernier, *Phys. Status Solidi* **60**, K23 (1973).

²²T. F. Gesell, E. T. Arakawa, M. W. Williams, and R. N. Hamm, *Phys. Rev. B* **7**, 5141 (1973).

²³R. P. Madden, in *Physics of Thin Films*, edited by G. Hass (Academic, New York, 1963), Vol. 1, p. 150.

²⁴H. Kanter, *Phys. Rev. B* **1**, 522 (1970).

²⁵B. D. Feuerbacher, R. B. Godwin, and M. Skibowski, *Z. Phys.* **224**, 172 (1969).

²⁶W. Pong, R. Sumida, and G. Moore, *J. Appl. Phys.* **41**, 1869 (1970).

²⁷T. Wooten, T. Huen, and R. N. Stuart, in *Optical Properties and Electronic Structure of Metals and Alloys*, edited by F. Abeles (North-Holland, Amsterdam, 1966), p. 333.

²⁸J. J. Quinn, *Phys. Rev.* **126**, 1453 (1962).

²⁹J. C. Ashley and R. H. Ritchie, *J. Phys. Chem. Solids* **26**, 1689 (1965).

³⁰L. Kleinman, *Phys. Rev. B* **3**, 2982 (1971).